

An Efficient Convex Hull-Based Vehicle Pose Estimation Method for 3D LiDAR

Ningning Ding¹, Ruihao Ming¹, Bo Wang¹, Yafei Gu¹

Abstract—Vehicle pose estimation is essential in the perception technology of autonomous driving. However, due to the different density distributions of the LiDAR point cloud, it is challenging to achieve accurate direction extraction based on 3D LiDAR by using the existing pose estimation methods. In this paper, we proposed a novel convex hull-based vehicle pose estimation method. The extracted 3D cluster is reduced to the convex hull, reducing the computation burden. Then a novel criterion based on the minimum occlusion area is developed for the search-based algorithm, which can achieve accurate pose estimation. The proposed algorithm is validated on the KITTI dataset and a manually labeled dataset acquired at an industrial park. The results show that our proposed method can achieve better accuracy than the three mainstream algorithms while maintaining real-time speed.

I. INTRODUCTION

Autonomous driving has drastically developed in the last decades. The safety of autonomous driving requires a reliable perception system to perceive surroundings for mobile platforms. In perception technology, 3D object detection is one of its main research directions, and numerous researchers have applied various 3D object detection [1], [2], [3], [4]. In particular, a 3D light detection and ranging (LiDAR) sensor has been extensively deployed to allow for centimeter-level accuracy, all-weather operation, and its ability to measure great distances compared with stereo cameras [5]. In this article, we specifically focus on 3D object detection based on LiDAR. 3D object detection based on LiDAR falls into two categories: traditional methods and deep learning methods. In recent years, various learning-based 3D object detection methods have been proposed, including VoxelNet [6], PointRCNN [7], PointPillars [8], CenterPoint [9], among others. Most of these approaches provide an end-to-end solution to 3D object detection based on a 3D convolutional neural network and exhibit outstanding performance. However, there are two inherent potential limitations. First, learning-based methods require labeling by humans, which is both severely laborious and time-consuming. Second, the performance of learning-based 3D object detection methods can be degraded when implemented in scenes different from the training dataset or sensor configurations. On the contrary, the adaptability of traditional methods is much better. In the traditional 3D object detection pipeline of 3D LiDAR, it is generally necessary to first perform ground segmentation with the original 3D point cloud and then perform point

cloud clustering with the non-ground point cloud. The 3D object detection task is finally completed after estimating the object's bounding box according to the clustering results. The main advantage of the traditional methods is that they do not need prior information about the environment for training. Thus, the generalization performance of the traditional method is better than the learning-based method.

The work in this paper focuses on estimating the vehicle's pose with the clustering point cloud in a LiDAR perception pipeline described above. The main contributions of this paper are listed as follows:

- We developed a convex hull-based vehicle pose estimation method for 3D LiDAR, a novel criterion based on the minimum occlusion area is employed, which can achieve better performance while maintaining real-time speed.
- Our proposed algorithm was evaluated with the KITTI dataset [13] and our own dataset. Experimental evidence corroborates the proposed algorithm exhibits promising performance compared with state-of-the-art methods.

II. RELATED WORK

The current vehicle pose estimation algorithms for 3D LiDAR based on traditional methods can be categorized into two types: pose estimation algorithms based on specific point cloud distribution shapes and global pose estimation algorithms. The pose estimation algorithms based on the point cloud distribution shapes are generally classified into L-shape, U-shape, and E-shape [15], [16]. Since the L-shape has appeared most often in the distribution of 3D LiDAR point clouds [11], many methods have used this feature to estimate the pose of objects. Zhang et al. [10] proposed a search-based method for pose estimation of the vehicle. It iterates all possible directions of the rectangle, and multiple criteria are applied to evaluate the optimal fitting directions. However, this method is computationally expensive, and is hard to achieve real-time speed when using complex criteria such as the variance criterion. Kim *et al.* [20] proposed an iterative end-point fitting method to extract L-shape features from a 3D point cloud. This method starts with the minimum and maximum clustering angle points as the end points of the baseline. The point that has the longest distance from the baseline to each point of the cluster is determined as the break-point. The final pose estimation bounding box was determined by extracting the farthest point from the baseline as the L-shaped corner point. However, this method assumes that all point clouds present a complete L-shape. To

¹Ningning Ding, Ruihao Ming, Bo Wang and Yafei Gu are with Jiangsu Jingling Institute of Intelligent Manufacturing Co., Ltd., China

overcome this limitation, Zhao *et al.* [11] proposed a new corner edge-based L-shape fitting method. After calculating the approximate corner point, it was further judged whether the point was the corner point of the L-shape or the side point of the vehicle. Then the RANSAC algorithm was used to fit the L-shape features to obtain the pose estimation result.

Compared to the pose estimation method based on some specific shape, a global-based pose estimation algorithm depends less on the point cloud's specific geometry and focuses more on the global applicability of the algorithm. In reference [17], the authors proposed an orientation-corrected bounding box fitting method based on the convex hull and a line creation heuristic. with the help of the rapidity features of convex hull extraction, this algorithm can efficiently perform correct pose estimation even when the point cloud was sparse. An *et al.* [18] proposed a vehicle pose estimation algorithm using a low-end 3D LiDAR. This algorithm first established four vehicle models with different observation angles, then modeled the vehicle's measured size as a uniformly distributed sample, and finally applied the idea of template matching to estimate the vehicle's pose. Yang *et al.* [19] proposed a new vehicle pose estimation method based on edge distance. The introduced edge distance describes the distribution of the point clouds well. Then the bounding rectangle based on the edge distance is used to estimate the vehicle's pose. Meanwhile, if the vehicle has only one visible side or the point clouds are sparse, the correction is used to modify the bounding rectangle to obtain a more accurate vehicle pose estimation.

III. METHODOLOGY

The proposed method consists of several steps to evaluate a candidate orientation for the vehicle, including convex hull extraction and score calculation. In this section, we will discuss the detailed implementation of the proposed algorithm, as well as its fundamentals.

Since we only care about the yaw angle of objects in the autonomous driver application, we can project the 3D point cloud onto the x-y plane. This reduces the original clusters from 3D space to 2D space and reduces the computational burden for the following steps. However, the projected 2D cluster lost the information along the z-axis. To get the height and position of the bounding box along the z-axis, we should calculate the minimum and maximum z values of the 3D cluster, namely z_{min} and z_{max} , before projection. The height of the bounding box equals $z_{max} - z_{min}$, and the position of the bounding box along the z-axis is $(z_{max} + z_{min})/2$. Then we need to extract the convex-hull points from the projected 2D cluster. For consideration of both simplicity and efficiency, we choose the Graham scan method [12] to generate a set of convex-hull points from the projected 2D point cloud.

The key issue of vehicle pose estimation when using a search-based algorithm is to choose the proper criterion to decide which orientation is the best option. There are already many criteria proposed in the literature, like area

minimization, closeness maximization, and variance minimization [10]. However, these criteria are only appropriate for the 2D cluster, and its performance will degrade when using a convex hull. This is due to some information being lost when reducing the 2D cluster into a convex hull. Besides, these criteria are mainly suitable when the cluster is an L-shape. However, due to occlusion and different viewing angles, the L-shape cannot be observed in some cases.

In this paper, we proposed a novel criterion based on the maximum driveable area. This is a straightforward idea since the wrong estimation of vehicle orientation will result in the driveable area being occupied by mistake. The goal of our criterion is to minimize this wrong occlusion region (OR), as presented by OR in Figure 1. It should be noted that the area of OR is hard to calculate if using the original 2D cluster. Fortunately, calculating the area of OR becomes possible after converting the 2D cluster to a convex hull.

Inspired by the concept of calculus, the area of OR can be divided into many trapezoids as shown in Figure 1. To achieve this, the first thing is to choose the appropriate projection line from the rectangle's four edges. Considering the point cloud distribution of lidar, we first calculate the corner point of the convex hull according to the minimum distance from the convex hull points to the origin of LiDAR. Then we calculate the distance of the rectangle's four corner points to the origin of LiDAR and rank them in descending order, the last two edges will be the candidate edge. Finally, we compare the candidate edges, and the longer one will be the projection line.

Inspired by the concept of calculus, the area of OR can be divided into many trapezoids as shown in Figure 1. To achieve this, the first thing is to choose the appropriate projection line from the rectangle's four edges. Considering the point cloud distribution of lidar, we first calculate the rectangle's corner point according to the minimum distance from the rectangle's four vertices to the origin of LiDAR. The two sides adjacent to the rectangle's corner points will be candidate projection edges. Finally, we compare the two candidate edges, and the longer one will be the projection line.

The next step is to calculate OR's area using the projection line. To simplify this problem, we calculate the corner point of the convex hull according to the minimum distance from the convex hull points to the origin of LiDAR. Then we make a cutting line perpendicular to the projection line through the corner point of the convex hull and separate OR into two parts. The part on the right side of the corner point is noted as OR_r , and another part is noted as OR_l . Then we can calculate these two regions' areas separately. Take the case in Figure 1 for example, the OR_r can be divided into 6 trapezoids. For the i-th trapezoid, its area can be calculated as

$$OR_{r,i} = [d(p_{r,i}, l_p) + d(p_{r,i-1}, l_p)] \cdot (\overrightarrow{p_{r,i}p_{r,i-1}} \cdot \overrightarrow{e_{l_p}}) / 2 \quad (1)$$

where $d(p_{r,i}, l_p)$ denotes the relative distance of $p_{r,i}$ to the projection line l_p , $\overrightarrow{e_{l_p}}$ is the unit direction vector of line l_p . It

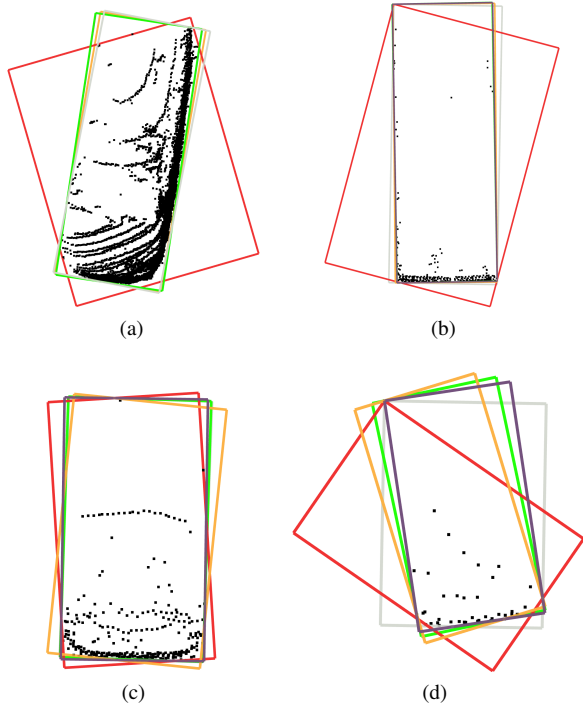


Fig. 3: Sample results of vehicle pose estimation on KITTI dataset. Green boxes from the ground truth, red boxes come from the PCA-based method, orange boxes come from the RANSAC-based method, gray boxes from the variance criterion, purple boxes from the closeness criterion, and blue boxes from the proposed algorithm.

will read the single object’s point cloud and calculate its orientation. It is worth noting that the orientation value in KITTI labels ranges from $-\pi$ to π . We convert it to the range of 0 to $\pi/2$ to be consistent with our algorithm. After comparing the estimated value with the ground truth information, we can get the pose estimation error.

The mean and standard deviation for the absolute orientation error are listed in Table I, in which the mean absolute error reflects the estimation accuracy. As shown in Table I, our proposed algorithm gets the best result in both mean value and standard deviation value. The L-shape fitting method with the closeness criterion is next only to our proposed algorithm. The PCA-based method has the worst performance, and the mean and stand deviation of absolute orientation error is larger than 10.

Table II presents the computation time fitting one object. Our proposed method takes much less than 1 ms to fit one object. If a 3D LiDAR operates at 10hz, our proposed method is capable of fitting more than 100 objects in real time. The STD value of the runtime is about half of the mean value, which shows that our proposed method is very stable. The PCA-based method is the fastest and is approximately one magnitude faster than our proposed method. The RANSAC-based method is closer to our proposed method and is also less than 1 ms. However, the STD value of the runtime is

TABLE I: Orientation error comparison between our proposed method and other vehicle pose estimation algorithm on KITTI Dataset

Methods	Mean (deg) ↓	STD (deg) ↓
PCA based	11.937	10.326
RANSAC based	4.280	6.785
L-shape Fitting (Variance)	6.158	7.980
L-shape Fitting (Closeness)	3.737	6.225
Proposed	1.815	4.107

TABLE II: Runtime comparison between our proposed method and other vehicle pose estimation algorithm on KITTI Dataset

Methods	Mean (ms) ↓	STD (ms) ↓
PCA based	0.027	0.063
RANSAC based	0.830	1.707
L-shape Fitting (Variance)	17.381	37.146
L-shape Fitting (Closeness)	17.346	36.349
Proposed	0.987	0.384

much larger than the mean value, which shows that our method is more stable than the RANSAC-based method. The mean running time of the L-shape fitting algorithm is larger than 17ms, which shows that this algorithm is time-consuming. Besides, the variance minimization criterion consumes more time because of the heavy computation in calculating the variance.

The examples of fitting results on the KITTI dataset are shown in Figure 3. In Figure 3(a),(b), the cluster is L-shape, and our method gets the best pose estimation result. The other method except for PCA-based also gets good results. The cluster in Figure 3(c) is not L-shape, our method still gives the best estimation result, and the RANSAC-based method can not gives the ideal result. In Figure 3(d), our proposed method is also valid even though the cluster is very sparse.

B. Own Dataset

Our own dataset is collected with a Velodyne Puck (VLP-16) 3D LiDAR in an industrial park, as shown in Figure 4. We labeled 420 frames of LiDAR point cloud using the 3D bounding box annotation tool: SUSTechPOINTS [14]. Then we convert these labels to the KITTI format. The rest procedures are the same as the KITTI dataset.

The mean and standard deviation for the absolute orientation error for our own dataset are listed in Table III. Comparing the KITTI dataset, the mean accuracy is higher. This is because the collected vehicle point cloud is closer to the LIDAR than the KITTI dataset, making it easy to estimate the vehicle’s pose. Table II presents the computation time fitting one object on our own dataset. Different from the KITTI dataset, the running time of all algorithms increases due to the collected vehicle point cloud is denser. However, the runtime of our proposed algorithm in our own dataset is closer to that in the KITTI dataset, which proves that our proposed method is not sensitive to the cluster’s point

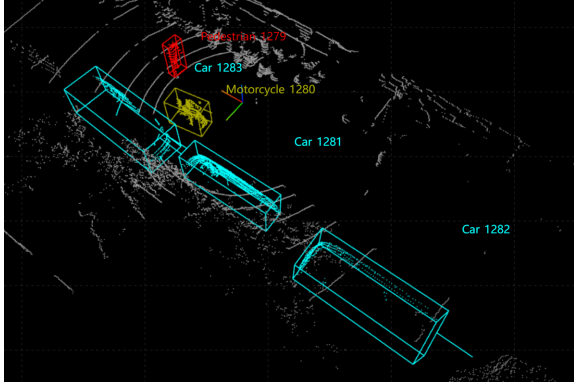


Fig. 4: A demonstration of our own dataset and its annotation.

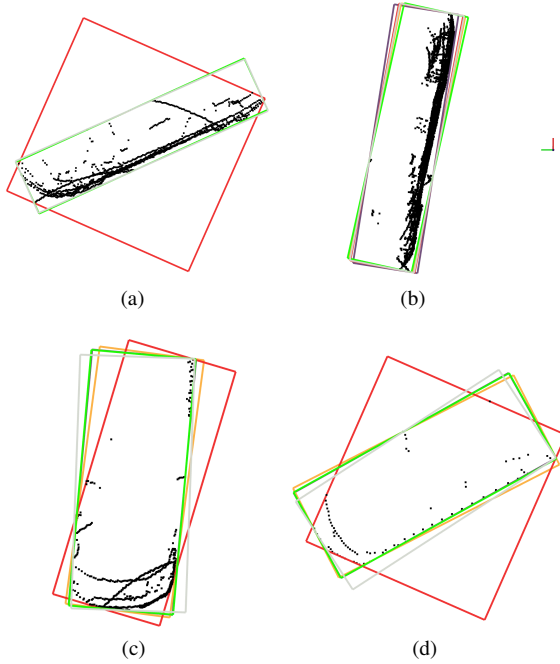


Fig. 5: Sample results of vehicle pose estimation on our own dataset. Green boxes from the ground truth, red boxes come from the PCA-based method, orange boxes come from the RANSAC-based method, gray boxes from the variance criterion, purple boxes from the closeness criterion, and blue boxes from the proposed algorithm.

cloud size. In contrast to our method, the RANSAC-based method has been increased to two times as compared with the KITTI dataset. The examples of fitting results on our own dataset are shown in Figure 5. Similar to the KITTI dataset, our proposed method can achieve excellent performance in various cases.

V. CONCLUSION

A novel convex hull-based vehicle pose estimation method is proposed in this paper. The convex hull extraction and the novel criterion based on the minimum occlusion area

TABLE III: Orientation error comparison between our proposed method and other vehicle pose estimation algorithms on our own dataset

Methods	Mean (deg) ↓	STD (deg) ↓
PCA based	11.959	9.941
RANSAC based	1.816	2.231
L-shape Fitting (Variance)	5.354	6.500
L-shape Fitting (Closeness)	3.691	5.867
Proposed	1.059	1.596

TABLE IV: Runtime comparison between our proposed method and other vehicle pose estimation algorithms on our own dataset

Methods	Mean (ms) ↓	STD (ms) ↓
PCA based	0.072	0.067
RANSAC based	2.068	2.458
L-shape Fitting (Variance)	38.215	32.252
L-shape Fitting (Closeness)	37.953	31.835
Proposed	1.351	0.301

make our algorithm achieve high pose estimation accuracy while maintaining real-time speed. Experimental results on the KITTI dataset and a manually labeled dataset show that the proposed method can estimate the vehicle's pose stably and accurately while maintaining real-time speed. In our future work, we will refine the projection line selection process to avoid some wrong estimation cases. The speed of our proposed method can be further reduced by applying parallelization.

REFERENCES

- [1] Y. Li, Z. Ge, G. Yu, J. Yang, Z. Wang, Y. Shi, J. Sun, and Z. Li, "Bevdepth: Acquisition of reliable depth for multi-view 3d object detection," *arXiv preprint arXiv:2206.10092*, 2022.
- [2] Y. Wang, B. Yang, R. Hu, M. Liang, and R. Urtasun, "Plumenet: Efficient 3d object detection from stereo images," in *2021 IEEE/RSJ International Conference on Intelligent Robots and Systems (IROS)*, pp. 3383–3390, IEEE, 2021.
- [3] X. Ma, W. Ouyang, A. Simonelli, and E. Ricci, "3d object detection from images for autonomous driving: a survey," *arXiv preprint arXiv:2202.02980*, 2022.
- [4] G. Zamanakos, L. Tsochatzidis, A. Amanatiadis, and I. Pratikakis, "A comprehensive survey of lidar-based 3d object detection methods with deep learning for autonomous driving," *Computers & Graphics*, vol. 99, pp. 153–181, 2021.
- [5] J. Behley, M. Garbade, A. Milioto, J. Quenzel, S. Behnke, C. Stachniss, and J. Gall, "Semantickitti: A dataset for semantic scene understanding of lidar sequences," in *Proceedings of the IEEE/CVF International Conference on Computer Vision*, pp. 9297–9307, 2019.
- [6] Y. Zhou and O. Tuzel, "Voxelnet: End-to-end learning for point cloud based 3d object detection," in *Proceedings of the IEEE conference on computer vision and pattern recognition*, pp. 4490–4499, 2018.
- [7] S. Shi, X. Wang, and H. Li, "Pointcnn: 3d object proposal generation and detection from point cloud," in *Proceedings of the IEEE/CVF conference on computer vision and pattern recognition*, pp. 770–779, 2019.
- [8] A. H. Lang, S. Vora, H. Caesar, L. Zhou, J. Yang, and O. Beijbom, "Pointpillars: Fast encoders for object detection from point clouds," in *Proceedings of the IEEE/CVF conference on computer vision and pattern recognition*, pp. 12697–12705, 2019.
- [9] T. Yin, X. Zhou, and P. Krahenbuhl, "Center-based 3d object detection and tracking," in *Proceedings of the IEEE/CVF conference on computer vision and pattern recognition*, pp. 11784–11793, 2021.

- [10] X. Zhang, W. Xu, C. Dong, and J. M. Dolan, "Efficient l-shape fitting for vehicle detection using laser scanners," in *2017 IEEE Intelligent Vehicles Symposium (IV)*, pp. 54–59, IEEE, 2017.
- [11] C. Zhao, C. Fu, J. M. Dolan, and J. Wang, "L-shape fitting-based vehicle pose estimation and tracking using 3d-lidar," *IEEE Transactions on Intelligent Vehicles*, vol. 6, no. 4, pp. 787–798, 2021.
- [12] R. L. Graham, "An efficient algorithm for determining the convex hull of a finite planar set," *Info. Pro. Lett.*, vol. 1, pp. 132–133, 1972.
- [13] A. Geiger, P. Lenz, C. Stiller, and R. Urtasun, "Vision meets robotics: The kitti dataset," *The International Journal of Robotics Research*, vol. 32, no. 11, pp. 1231–1237, 2013.
- [14] E. Li, S. Wang, C. Li, D. Li, X. Wu, and Q. Hao, "Sustech points: A portable 3d point cloud interactive annotation platform system," in *2020 IEEE Intelligent Vehicles Symposium (IV)*, pp. 1108–1115, IEEE, 2020.
- [15] F. Xu, H. Liang, Z. Wang, L. Lin, and Z. Chu, "A real-time vehicle detection algorithm based on sparse point clouds and dempster-shafer fusion theory," in *2018 IEEE International Conference on Information and Automation (ICIA)*, pp. 597–602, IEEE, 2018.
- [16] D. Wittmann, F. Chucholowski, and M. Lienkamp, "Improving lidar data evaluation for object detection and tracking using a priori knowledge and sensorfusion," in *2014 11th International Conference on Informatics in Control, Automation and Robotics (ICINCO)*, vol. 1, pp. 794–801, IEEE, 2014.
- [17] B. Naujoks and H.-J. Wuensche, "An orientation corrected bounding box fit based on the convex hull under real time constraints," in *2018 IEEE Intelligent Vehicles Symposium (IV)*, pp. 1–6, IEEE, 2018.
- [18] J. An and E. Kim, "Novel vehicle bounding box tracking using a low-end 3d laser scanner," *IEEE Transactions on Intelligent Transportation Systems*, vol. 22, no. 6, pp. 3403–3419, 2020.
- [19] J. Yang, G. Zeng, W. Wang, Y. Zuo, B. Yang, and Y. Zhang, "Vehicle pose estimation based on edge distance using lidar point clouds (poster)," in *2019 22th International Conference on Information Fusion (FUSION)*, pp. 1–6, IEEE, 2019.
- [20] D. Kim, K. Jo, M. Lee, and M. Sunwoo, "L-shape model switching-based precise motion tracking of moving vehicles using laser scanners," *IEEE Transactions on Intelligent Transportation Systems*, vol. 19, no. 2, pp. 598–612, 2017.